JOURNAL OF AIRCRAFT
Vol. 38, No. 3, May–June 2001

Microblowing for High-Angle-of-Attack Vortex Flow Control on a Fighter Aircraft

Frederick W. Roos*
The Boeing Company, St. Louis, Missouri 63166

Effectiveness of the microblowing technique for controlling forebody vortex asymmetry at high angles of attack has been investigated in low-speed wind-tunnel experiments with the F-15E fighter aircraft configuration. One blowing-port installation, based on previous experiments with generic forebody shapes, was evaluated. At very high angles of attack (α >50 deg), microblowing was effective in generating and controlling yawing moment levels comparable to those demonstrated by high-pressure jet nozzle blowing, while requiring only $\frac{1}{100}$ as much mass flow, demonstrating the leveraging available through controlling the vortex flowfield at the point of instability. The microblowing port configuration employed was unable to generate usable yawing moments at moderate angles of attack ($\alpha \leq 35$ deg). Control-port optimization promises to improve microblowing effectiveness in the intermediate α range.

Nomenclature

A	=	reference area for all coefficients: forebody planform area for isolated forebody; wing planform area for F-15
$C_{\dot{m}}$	=	control-jet mass-flow-rate coefficient, $C_{\dot{m}} = \dot{m}_j/\rho_\infty U_\infty A$
C_N	=	normal force coefficient
C_n	=	yawing-moment coefficient
C_Y	=	side-force coefficient
D	=	base diameter of F-15E model forebody
d	=	diameter of control-jet orifice
F_Y	=	side force
$\dot{m}_j$	=	mass-flow rate of control jet
Re	=	Reynolds number based on D, $U_\infty D/\nu_\infty$
T	=	equivalent sonic-jet thrust
U_∞	=	freestream flow speed
x	=	axial distance from (virtual) apex of tangent ogive forebody
α	=	angle of attack
β	=	sideslip angle
ν_∞	=	kinematic viscosity of freestream air
ρ_∞	=	freestream air density
ϕ	=	azimuthal angle (from windward meridian)
ψ	=	yaw angle

Introduction

SLENDER bodies of revolution, especially those with pointed noses, develop nonlinear lift forces as well as very large side forces at high angles of attack α; these characteristics are associated with asymmetry of the vortex system formed by flow separation on the leeward side of such bodies.[1] In recent years a great deal of effort has gone into attempts to suppress and control slender-body vortex-flow asymmetry at high α, motivated primarily by the quest for enhanced controllability and maneuverability of high-performance combat aircraft.[2] Excellent recent reviews of this activity can be found in papers by Malcolm[3] and Williams.[4]

One of the more promising approaches to forebody vortex-asymmetry management is pneumatic control, i.e., blowing, as originally developed by Skow and Peake.[5] A variation of the pneumatic-control approach is a very low-mass-flow technique known as *microblowing*, where very slight blowing through one of two symmetrically placed, forward-facing orifices very close to the forebody tip, controllably manipulates the asymmetry state of the forebody vortices. The microblowing technique, which was first developed in combination with the use of bluntness to suppress inherent asymmetry,[6] benefits from the substantial leverage to be derived from controlling the flow at the point of flow instability. (It has long been known that minute nose-shape details are responsible for triggering the instability that leads to asymmetric vortex configurations.[7])

The approach embodied in microblowing is sketched in Fig. 1. The local displacement effect of slight blowing through a jet on one side of the nose promotes detachment of the separated-flow vortex on that side of the forebody, leading to a side force toward the opposite side. Initial low-speed results obtained with the blunted 3.5-caliber tangent ogive forebody shape showed substantial response, as seen in Fig. 2 (Ref. 6), which indicates the basic characteristics of the low-energy pneumatic control. Within a range about $C_{\dot{m}} = 0$ (where $C_{\dot{m}} = \dot{m}_j/\rho_\infty U_\infty A$, with $\dot{m}_j =$ control-jet mass-flow rate, $+$ for right jet and $-$ for left, and $A =$ planform area of tangent-ogive forebody shape), the effect of blowing is proportional to $C_{\dot{m}}$, up to limiting levels of ΔC_Y (with different maxima for each α; also dependent on state of separating boundary layers, i.e., laminar or turbulent).

Levy et al.[8] have recently produced computational fluid dynamics simulations of high-α asymmetric flow about a 3.5-caliber tangent ogive (with a cylindrical afterbody) that lend substantial support to the argument that displacement effects are responsible for the controlled flow asymmetry produced by microblowing. In these simulations a small geometric "bump" was incorporated into the forebody nose close to the apex. The degree of vortex-flow asymmetry developed was found to increase as the height of the bump was increased, until a maximum effect was reached.[8] When the forces acting on the tangent ogive forebody alone were computed, the C_Y variation with bump size showed characteristics analogous to the microblowing results in Fig. 2 (Levy, Y., unpublished data, 1995).

The leveraging effect available through microblowing can be appreciated if the side force F_Y corresponding to the maximum response level indicated in Fig. 2 is compared to, say, the thrust T produced by a sonic-velocity reaction-control jet having a mass flow corresponding to the level of $C_{\dot{m}}$ providing maximum response (Fig. 2). Using appropriate values from Fig. 2 leads to

$$F_Y/T \approx 680$$

i.e., through manipulation of the flow instability, the microblowing technique produces a lateral force that is 680 times the equivalent thrust of the corresponding reaction-control jet.

Presented as Paper 96-0543 at the 34th Aerospace Sciences Meeting, Reno, NV, 15–18 January 1996; received 30 January 1999; revision received 18 August 1999; accepted for publication 8 September 2000.

*Senior Principal Technical Specialist, Active Flow Control Group, P.O. Box 516. Associate Fellow AIAA.

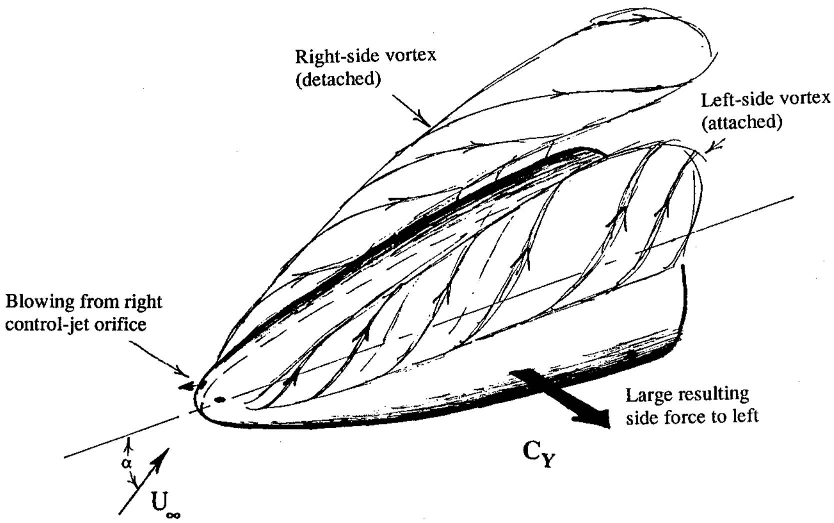

Fig. 1 Effect of forward-blowing control jets in triggering separated-flow asymmetry on blunted tangent ogive forebody.

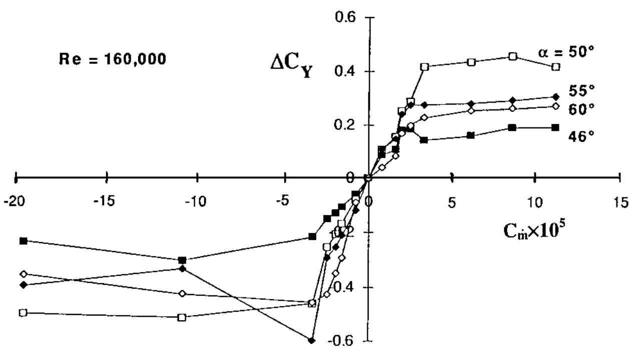

Fig. 2 Microblowing side-force control on blunted tangent ogive (laminar separation).

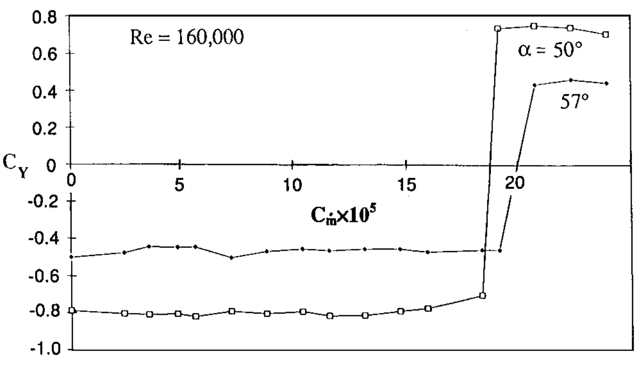

Fig. 3 Microblowing effectiveness on pointed tangent ogive (laminar separation).

Extension of the application of microblowing from the original blunted tangent ogive forebody to the unblunted (pointed) tangent ogive[9] produced the results shown in Fig. 3, which indicate the level of blowing $C_{\dot{m}}$ needed to overcome the inherent vortex-asymmetry characteristics of the pointed body. Adjusting for this initial offset permits comparison of blowing-effectiveness curves for the pointed and blunted tangent ogives at $\alpha = 50$ deg (Fig. 4). The pointed forebody with forward-blowing control jets develops side-force-control characteristics comparable to the blunted forebody. The trend suggests greater extremes of C_Y and greater sensitivity to blowing rate with reduced nose bluntness.

The present paper reports results of exploratory wind-tunnel tests of an application of the microblowing technique to a fighter-aircraft configuration.

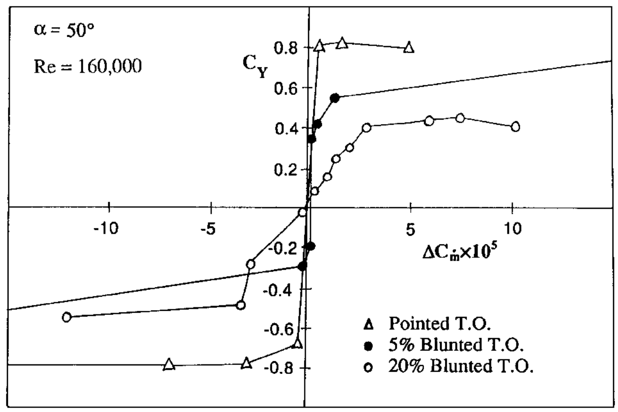

Fig. 4 Microblowing effectiveness on blunted and pointed forebodies (laminar separation).

Experiments

Microblowing effectiveness was evaluated in a brief, preliminary experiment during a joint U.S. Air Force/NASA study of F-15 high-alpha forebody vortex control via above-moldline jet nozzle blowing.[10] A 10%-scale F-15E model was used for the low-speed tests, which were conducted in the NASA Langley 30- × 60-ft Tunnel (Fig. 5). Aerodynamic forces and moments were measured by an internal strain-gauge balance. A replacement nose incorporating a pair of symmetrically placed, forward-facing flush jet orifices was designed and constructed to mate with the existing full-configuration F-15E model. The control-jet installation, which was based on the earlier tangent-ogive model experience, is shown in Fig. 6. No variations in jet orifice location or pointing direction were studied. The flush, forward-facing orifices were positioned at an axial station $x/D = 0.12$ aft of the nose tip, where $D =$ base diameter of the F-15E model forebody, and were azimuthally located at ±45 deg around the nose (from the top centerline). Because the earlier studies had revealed that the displacement effect of the control-jet flow was the instability-triggering mechanism, control-jet orifice diameter d was made sufficiently large ($d/D = 0.017$) to ensure subsonic flow at all mass-flow rates. The present tests were all run at a freestream flow speed $U_\infty = 82$ fps, which corresponds to a Reynolds number, based on D, of $Re = 2 \times 10^5$, well within the range for laminar crossflow separation on the forebody. Clean, dry shop air at very low pressure was supplied to the control-jet orifices via flexible lines that produced no measurable balance bridging. Microblowing mass-flow rates were manually set using a calibrated floating-ball flow meter. Additional details of model pneumatic plumbing installation and tunnel test procedures are found in Ref. 10.

Fig. 5 10% scale F-15E model in NASA Langley 30-by 60-ft Wind Tunnel.

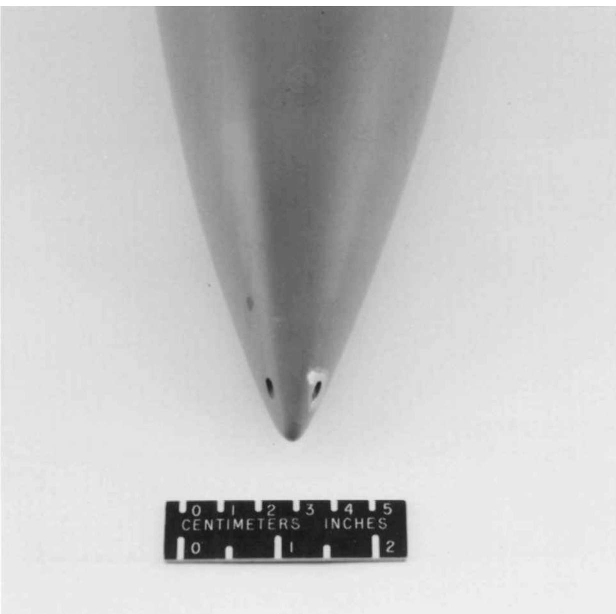

Fig. 6 Top view of microblowing control-jet configuration in nose of model F-15 radome.

Results

The basic microblowing performance results are shown in Fig. 7, in terms of yawing moment coefficient, C_n, variation with α at several blowing rates, $C_{\dot m}$, where $C_{\dot m} = \dot m_j / \rho_\infty U_\infty S_w$, with $\dot m_j$ = control-jet mass-flow rate (as before) and S_w = wing area. The baseline ($C_{\dot m} = 0$) case shows nonzero C_n for $\alpha \geq 48$ deg, a peculiarity of the nose shape on this particular F-15E model that was identified previously.[10] Interestingly, the onset α for the appearance of vortex asymmetry (as evidenced by $C_n \neq 0$) is consistent with Keener and Chapman's rule-of-thumb that the onset α is approximately twice the half-angle at the forebody apex[11] *if* account is taken of the F-15 forebody droop angle of ~5 deg. It is evident in Fig. 7 that, at least for α in the range where vortex system instability exists (i.e., for $\alpha \geq$ ~40 deg), microblowing can effectively counter the prevailing flow asymmetry and even reverse it. The effect is maximum at $\alpha = 60$ deg.

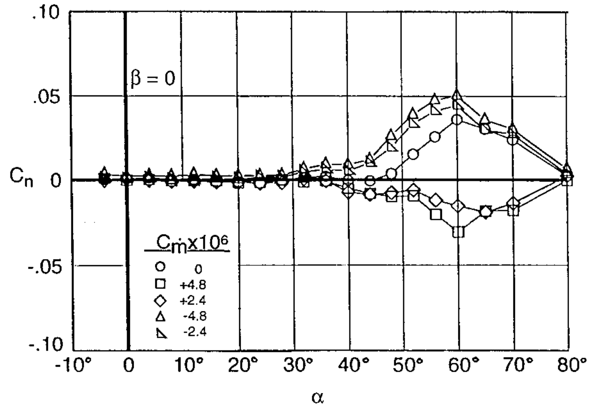

Fig. 7 High-α yawing moment generated with microblowing vortex control.

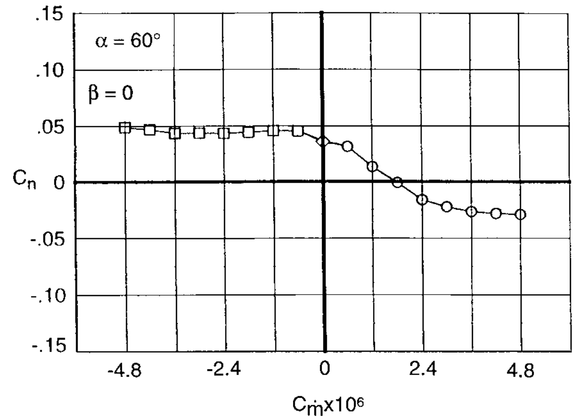

Fig. 8 Proportionality of yawing moment to microblowing mass-flow rate ($\alpha = 60$ deg).

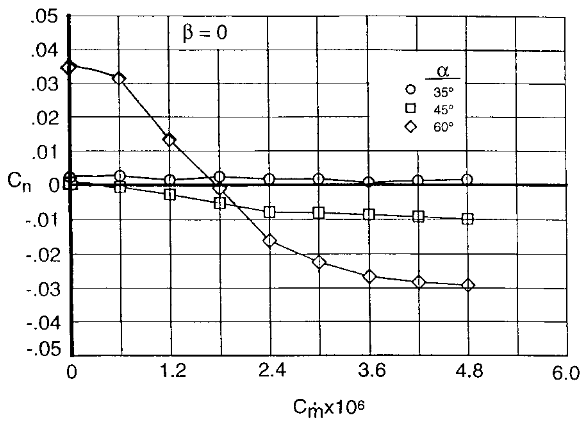

Fig. 9 Microblowing effectiveness for several α.

Data repeatability checks defined an uncertainty of ±0.001 in C_n measurements, whereas flow-meter reading uncertainty combined with relative calibration precision gave $C_{\dot m}$ accuracy of $\pm 0.025 \times 10^{-6}$.

Cross plotting of the $\alpha = 60$ deg results vs $C_{\dot m}$ (+ for right-side blowing, − for left) shows the effectiveness of microblowing yaw control and identifies the anticipated proportional-effect range (Fig. 8). Single-sided blowing results for several α (Fig. 9) show only minimal response to microblowing at $\alpha = 45$ deg and no meaningful effect at all for $\alpha = 35$ deg.

It is instructive to compare the yawing-moment-generation capabilities of microblowing with the above-surface nozzle blowing

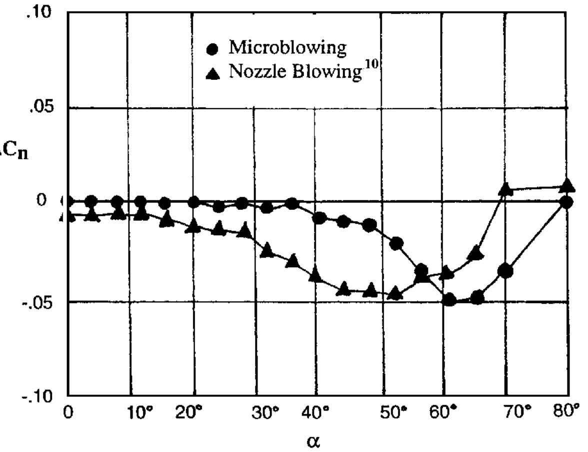

Fig. 10 Comparison of microblowing and above-moldline nozzle blowing (Ref. 10) yawing moments.

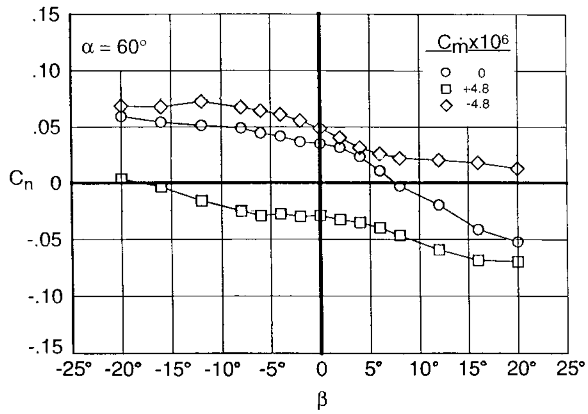

Fig. 11 Robustness of microblowing effectiveness across sideslip range.

method that has been developed.[10] Using ΔC_n to accommodate nose-to-nose variations in baseline C_n, the $C_{\dot{m}} = 4.8 \times 10^{-6}$ microblowing data from Fig. 7 are compared with low-rate nozzle-blowing data (from Fig. 15 of Ref. 10) in Fig. 10. Although the microblowing approach was unable to match the nozzle-blowing system in developing significant C_n in the intermediate α range, at higher α where it is effective, microblowing achieves comparable results with $\frac{1}{100}$ of the mass-flow rate, at substantially lower pressures. Considering the results of the forebody asymmetric-nose-bump experiments done by Moskovitz et al.,[12] as well as our own forebody-alone microblowing experiments,[6] it appears quite possible that azimuthal and/or axial repositioning of the microblowing control-jet orifices might improve the intermediate-α effectiveness; it was not possible to explore this prospect in the context of the experiments reported here.

As was demonstrated for nozzle-blowing vortex control,[7] the microblowing yawing-moment response holds up well across a substantial sideslip range (Fig. 11).

Conclusions

Low-speed wind-tunnel experiments have been conducted to study the effectiveness of microblowing, a low-energy pneumatic technique for controlling forebody vortex asymmetry at high angles of attack, applied to a full fighter aircraft configuration. The following primary conclusions were drawn:

1) At very high angles of attack ($\alpha > 50$ deg), microblowing was effective in generating and controlling significant yawing moments.

2) The microblowing port configuration employed was unable to generate usable yawing moment at moderate angles of attack ($\alpha \leq 35$ deg).

3) Yawing-moment levels developed at high α were comparable to those previously demonstrated by high-pressure jet nozzle blowing, while requiring only $\frac{1}{100}$ as much mass flow.

Acknowledgments

This research was conducted under the Boeing (McDonnell Douglas at the time) Independent Research and Development program. The author would like to thank Russ Osborn of Wright Labs and Sue Grafton of NASA Langley Research Center for the opportunity to evaluate microblowing in these experiments. He also acknowledges the assistance and support during the testing provided by Rick Boalbey of McDonnell Douglas, Ken Iwanski of Wright Labs, and Matt O'Rourke of Lockheed Engineering and Science Company.

References

[1]Allen, H. J., and Perkins, E. W., "A Study of the Effects of Viscosity on Flow over Slender Inclined Bodies of Revolution," NACA TR 1048, 1951.

[2]Skow, A. M., and Erickson, G. E., "Modern Fighter Aircraft Design for High-Angle-of-Attack Maneuvering," *High Angle-of-Attack Aerodynamics*, AGARD LS-121, March 1982, pp. 4.1–4.59.

[3]Malcolm, G. N., "Forebody Vortex Control—A Progress Review," AIAA Paper 93-3540, Aug. 1993.

[4]Williams, D. R., "A Review of Forebody Vortex Control Scenarios," AIAA Paper 97-1967, June 1997.

[5]Skow, A. M., and Peake, D. J., "Control of the Forebody Vortex Orientation by Asymmetric Air Injection," *Special Course on Aerodynamic Characteristics of Controls*, AGARD Rept. 711, July 1983.

[6]Roos, F. W., and Magness, C. L., "Bluntness and Blowing for Flowfield Asymmetry Control on Slender Forebodies," AIAA Paper 93-3409, Aug. 1993.

[7]Pick, G. S., "Investigation of Side Forces on Ogive-Cylinder Bodies at High Angles of Attack in the $M = 0.5$ to 1.1 Range," AIAA Paper 71-570, June 1971.

[8]Levy, Y., Hesselink, L., and Degani, D., "A Systematic Study of the Correlation Between Geometrical Disturbances and Flow Asymmetries," AIAA Paper 95-0365, Jan. 1995.

[9]Roos, F. W., "Low-Energy Pneumatic Control of Forebody Vortices," NASA CP-10143, Vol. 3, July 1994.

[10]Iwanski, K. P., and O'Rourke, M. J., "F-15 Forebody Vortex Flow Control Using Jet Nozzle Blowing," AIAA Paper 95-1800, June 1995.

[11]Keener, E. R., and Chapman, G. T., "Onset of Aerodynamic Side Forces at Zero Sideslip on Symmetric Forebodies at High Angles of Attack," AIAA Paper 74-770, Aug. 1974.

[12]Moskovitz, C. A., Hall, R. M., and DeJarnette, F. R., "Effects of Surface Perturbations on the Asymmetric Vortex Flow over a Slender Body," AIAA Paper 88-0483, Jan. 1988.